Electronic Supplementary Material (ESI) for Journal of Materials Chemistry A.

Supporting Information

Multi-functional composite nitrogen carrier for ammonia production via chemical looping route

Sheng Feng, † [ab] Wenbo Gao, † [b] Qianru Wang, [b] Yeqin Guan, [b] Hanxue Yan, [b] Han Wu, [b] Hujun Cao,* [b] Jianping Guo* [b] and Ping Chen [ab]

a. Zhang Dayu School of Chemistry, Dalian University of Technology, Dalian, China.

b. Dalian National Laboratory for Clean Energy, State Key Laboratory of Catalysis, Collaborative Innovation Center of Chemistry for Energy Materials, Dalian Institute of Chemical Physics, Chinese Academy of Sciences, Dalian, China.

† These authors have contributed equally.

*e-mail: guojianping@dicp.ac.cn and caohujun@dicp.ac.cn

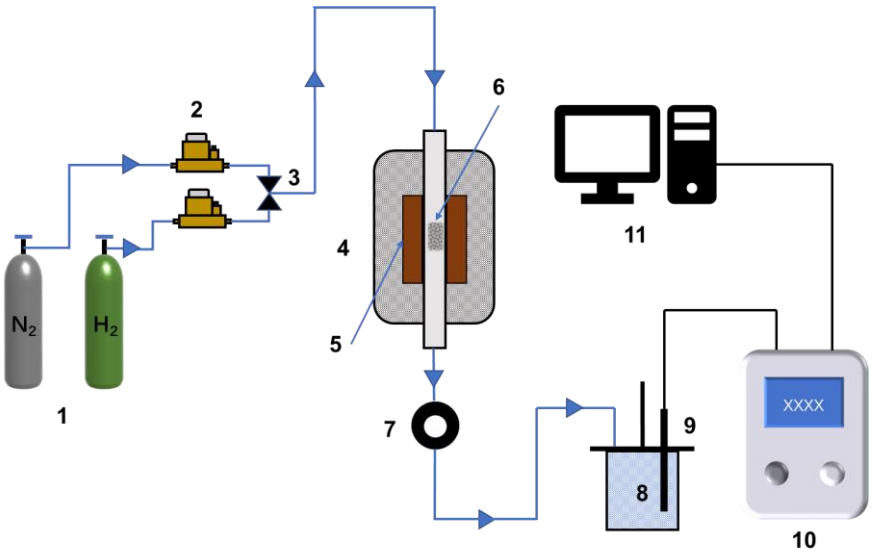

Fig. S1. The diagram of evaluation system for chemical looping ammonia synthesis. 1:gas cylinder, 2:mass flowmeter, 3: four-way valve, 4: reactor, 5: heating block, 6: N carrier materials, 7: counterbalance valve, 8: diluted sulfuric acid solution, 9: electrode, 10: conductivity meter, 11: computer.

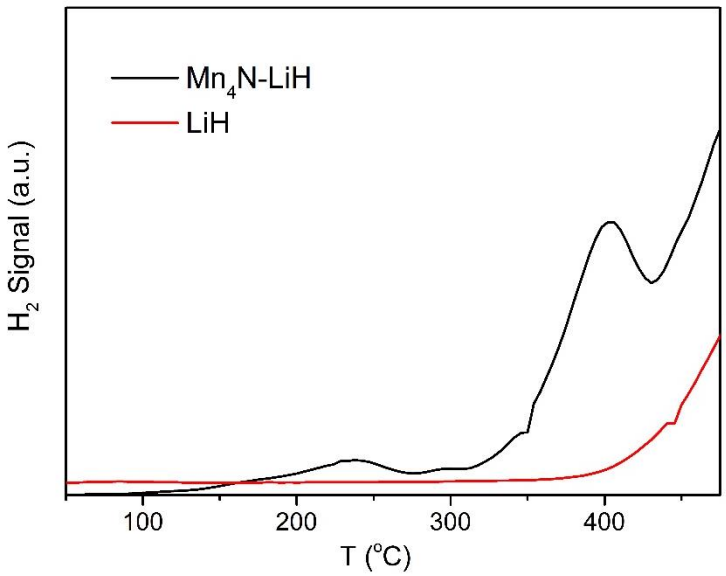

Fig. S2. N_2-TPR-MS profiles of LiH and Mn_4N-LiH samples. N_2 flow rate – 30 ml min^{-1}, ramping rate – 5 °C min^{-1}. The data of LiH was taken from ref. [1].

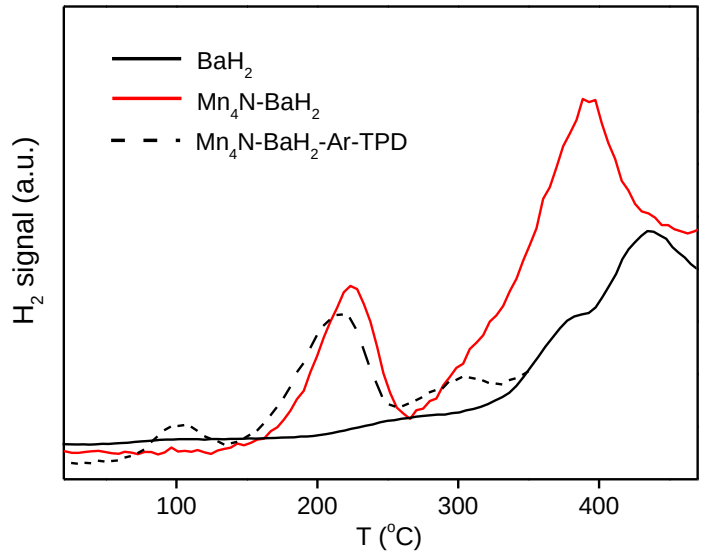

Fig. S3. N_2-TPR-MS profiles of BaH_2 and Mn_4N-BaH_2 samples (solid lines), and Ar-TPD-MS profile of Mn_4N-BaH_2 (dashed line). It is clearly seen that the reaction of N_2 and BaH_2 is much easier with the presence of Mn_4N. The N_2-TPR-MS profile of Mn_4N-BaH_2 shows two apparent H_2 peaks which are centered around 220 and 390 °C, respectively. By comparing with Ar-TPD-MS profile, it could be concluded that the H_2 peak at around 220 °C corresponds to the interaction between Mn_4N and BaH_2. The peak around 390 °C is mainly due to the fixation of N_2, which is at least 50 °C lower than that of BaH_2. N_2 or Ar flow rate – 30 ml min^{-1}, ramping rate – 5 °C min^{-1}. The data of BaH_2 were taken from ref. [1].

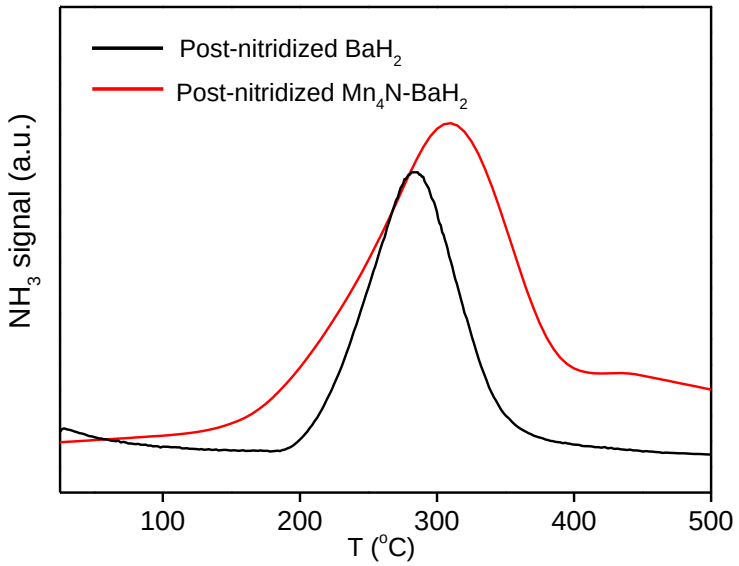

Fig. S4. H_2-TPR-MS profiles of post-nitridized BaH_2 (i.e., BaNH) and Mn_4N-BaH_2 samples. H_2 flow rate – 30 ml min^{-1}, ramping rate – 5 °C min^{-1}. The data of BaH_2 was taken from ref. [1].

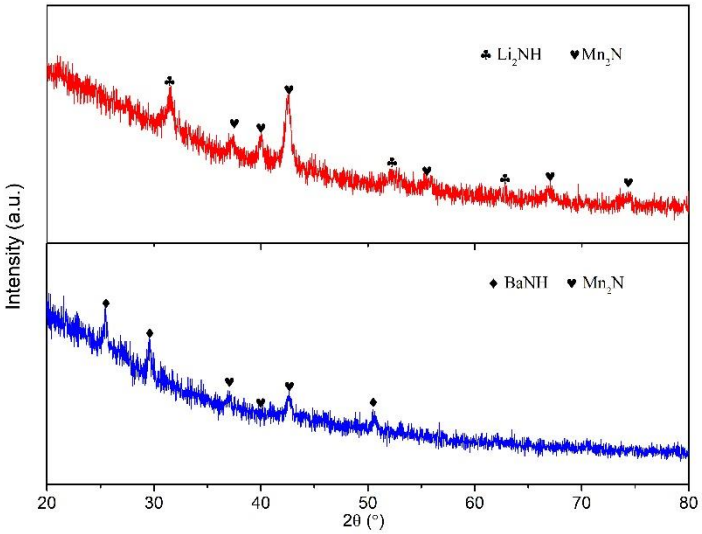

Fig. S5. XRD patterns of Mn_4N-LiH and Mn_4N-BaH_2 samples collected after second nitridation step.

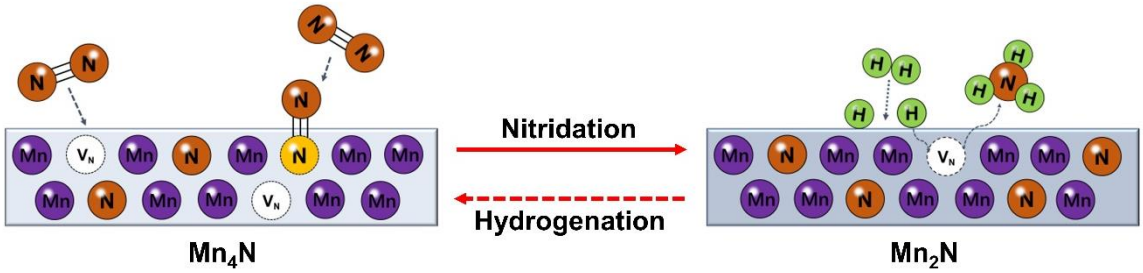

Fig. S6. Schematic diagram of CLAS mediated by Mn nitride. The nitrogen vacancies (V_N) may function as the active site for the activation and dissociation of N_2 molecules.

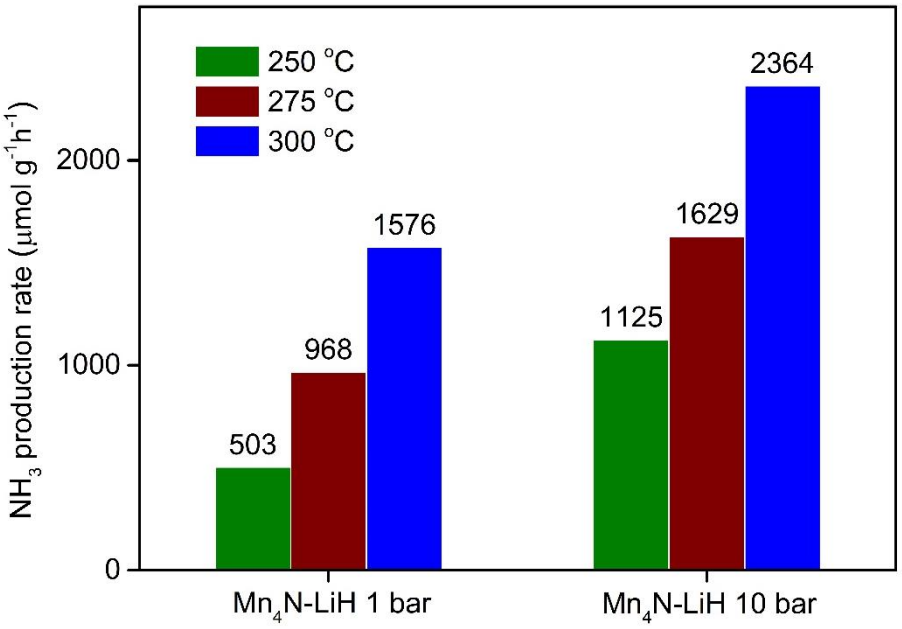

Fig. S7. NH_3 production rates of Mn_4N-LiH under 1 bar and 10 bar of pressure, respectively. Reaction conditions: WHSV = 60000 ml g^{-1} h^{-1}.

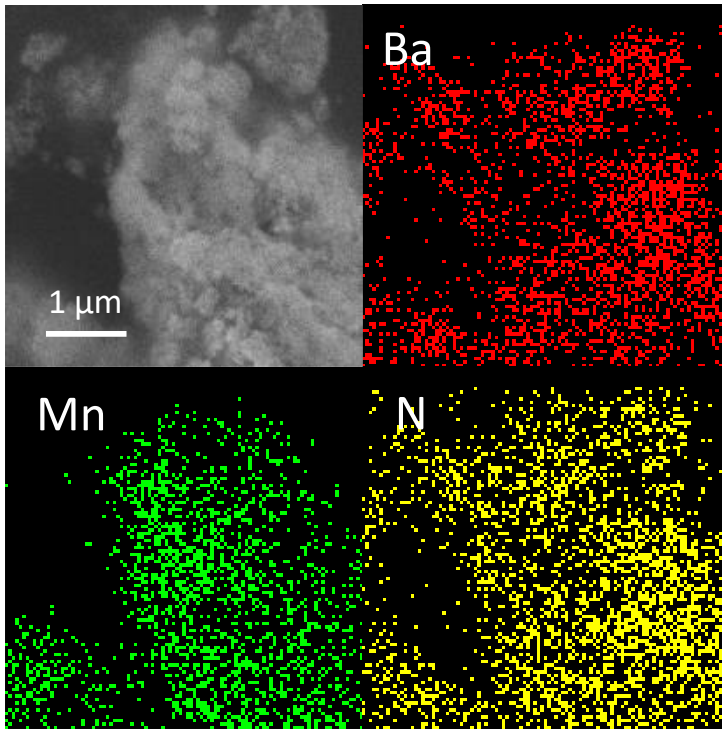

Fig. S8. SEM and elemental mapping images of the nitridized Mn_4N-BaH_2 sample.

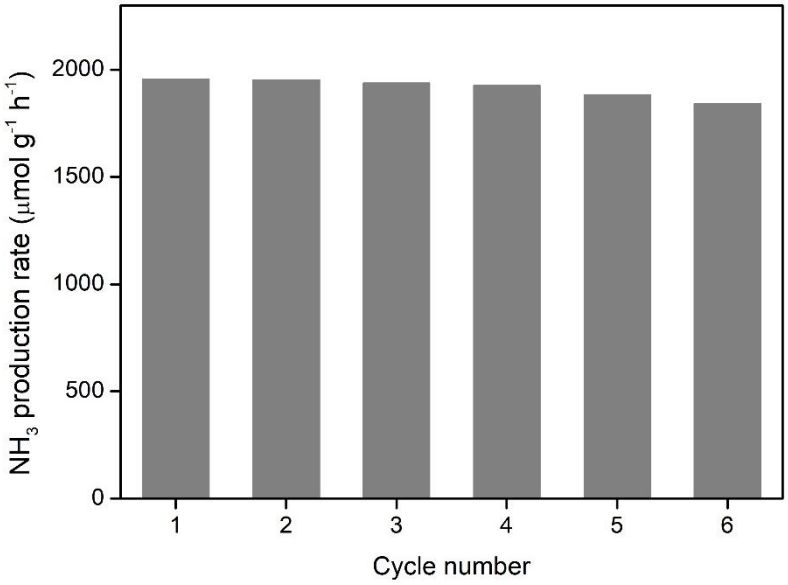

Fig. S9. Cyclic test of Mn_4N-BaH_2 sample for chemical looping ammonia synthesis at 275 ℃ and 1 bar of N_2 and H_2.

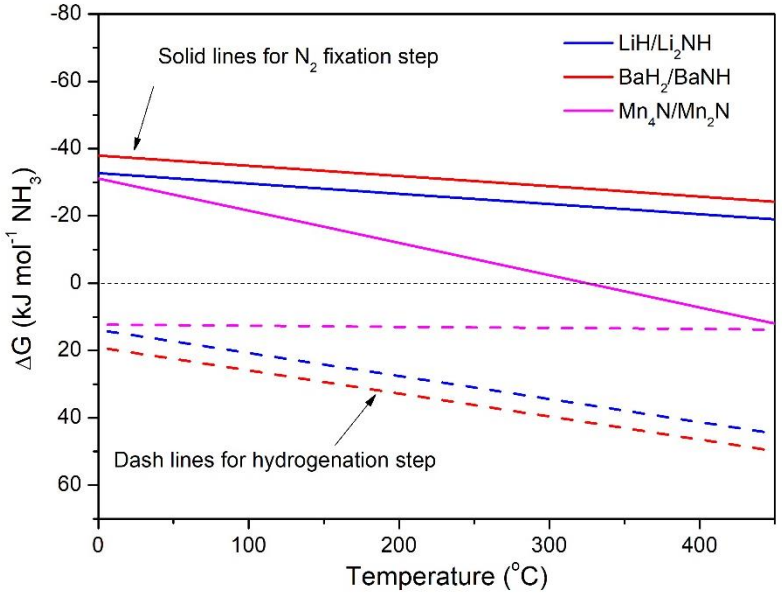

Fig. S10. Thermodynamic analyses of N_2 fixation and hydrogenation steps for LiH/Li_2NH, $BaH_2/BaNH$ and Mn_4N/Mn_2N pairs. The solid lines are the temperature dependences of ΔG for N_2 fixation over BaH_2, LiH and Mn_4N forming BaNH, Li_2NH and Mn_2N, respectively. The dashed lines are the temperature dependences of ΔG for hydrogenation of BaNH, Li_2NH and Mn_2N. The entropies of solids are not considered. The thermodynamic data used in this figure are given in Tables S1 and S2.

Table S1. Thermodynamic calculations of the nitridation of AH and Mn_4N. The entropies of solids are not considered. The standard enthalpies of formation (Δ_fH^o) of Li_2NH (ref. [2]) and BaNH (ref.[3]) are taken from the literatures. The standard enthalpies of formation of other substances are taken from "NIST Standard Reference Database Number 69". [4]

Reaction	2LiH	+	1/2N_2	→	Li_2NH	+	1/2H_2	Δ_rH^o (kJ mol^{-1})	Δ_rS^o (J mol^{-1} K^{-1})
Δ_fH^o (kJ mol^{-1})	-90.5		0		-222		0	-41	---
S^o (J mol^{-1} K^{-1})	---		191.6		---		130.7	---	-30.5
Reaction	BaH_2	+	1/2N_2	→	BaNH	+	1/2H_2	Δ_rH^o (kJ mol^{-1})	Δ_rS^o (J mol^{-1} K^{-1})
Δ_fH^o (kJ mol^{-1})	-178.7		0		-224.9		0	-46.2	---
S^o (J mol^{-1} K^{-1})	---		191.6		---		130.7	---	-30.5
Reaction	Mn_4N	+	1/2N_2	→	$2Mn_2N$			Δ_rH^o (kJ mol^{-1})	Δ_rS^o (J mol^{-1} K^{-1})
Δ_fH^o (kJ mol^{-1})	-128.7		0		-93			-57.3	---
S^o (J mol^{-1} K^{-1})	0		191.6		0			---	-95.8

Table S2. Thermodynamic calculations of the hydrogenation of ANH and Mn_2N. The entropies of solids are not considered.

Reaction	Li_2NH	+	$2H_2$	→	2LiH	+	NH_3	Δ_rH^o (kJ mol^{-1})	Δ_rS^o (J mol^{-1} K^{-1})
Δ_fH^o (kJ mol^{-1})	-222		0		-90.5		-45.9	-4.9	---
S^o (J mol^{-1} K^{-1})	---		130.7		---		192.8	---	-68.6
Reaction	BaNH	+	$2H_2$	→	BaH_2	+	NH_3	Δ_rH^o (kJ mol^{-1})	Δ_rS^o (J mol^{-1} K^{-1})
Δ_fH^o (kJ mol^{-1})	-224.9		0		-178.7		-45.9	0.3	---
S^o (J mol^{-1} K^{-1})	---		130.7		---		192.8	---	-68.6
Reaction	$2Mn_2N$	+	$3/2H_2$	→	Mn_4N	+	NH_3	Δ_rH^o (kJ mol^{-1})	Δ_rS^o (J mol^{-1} K^{-1})
Δ_fH^o (kJ mol^{-1})	-93		0		-128.7		-45.9	11.4	---
S^o (J mol^{-1} K^{-1})	---		130.7		0		192.8	---	-3.25

References

1. W. Gao, J. Guo, P. Wang, Q. Wang, F. Chang, Q. Pei, W. Zhang, L. Liu and P. Chen, *Nat. Energy*, 2018, **3**, 1067-1075.
2. P. Chen, Z. Xiong, J. Luo, J. Lin and K. L. Tan, *Nature*, 2002, **420**, 302-304.
3. A. P. Altshuller, *J. Chem. Phys.*, 1955, **23**, 1561-1562.
4. NIST Standard Reference Database Number 69. National Institute of Standards and Technology (2017) https://webbook.nist.gov/chemistry/.